




Ballistic long bone fracture pattern: an experimental study

Nathalie Schwab^{1,2} · Xavier Jordana^{1,3} · Jordi Monreal⁴ · Xavier Garrido⁴ · Joan Soler⁴ · Manel Vega⁴ · Pedro Brillas⁵ · Ignasi Galtés^{2,6} 

Received: 23 October 2023 / Accepted: 9 February 2024 / Published online: 20 February 2024
© The Author(s), under exclusive licence to Springer-Verlag GmbH Germany, part of Springer Nature 2024

Abstract

When dealing with badly preserved cadavers or skeletal human remains, the assessment of death circumstances remains challenging. When forensic evidence cannot be taken from the skin and soft tissue, the information may only be deduced from more resistant elements such as bone. Compared to cranial gunshot injuries, reliable data on ballistic long bone trauma remains scarce. This study aims to define ballistic fracture characteristics in human long bones. The shaft of 16 femurs and 13 humeri from body donors was perpendicularly shot with a 9-mm Luger full metal jacket bullet at an impact velocity of 360 m/s from a distance of 2 m. Some bones were embedded in Clear Ballistics Gel®, and some were shot without soft tissue simulant in order to better visualise the fracture propagation on the high-speed camera. The fractures were examined macroscopically and compared between the sample groups. We consistently found comminuted fractures with a stellate pattern. Fracture details were classified into entrance, exit and general characteristics. For some traits, we detected different occurrence values in the group comparison. The results indicate that some of the traits depend on bone properties such as shaft diameter, bone length and cortical thickness. The presence of ballistic gel also influenced some fracture traits, emphasising the relevance of soft tissue simulant in osseous gunshot experiments. This study revealed new insights in the detailed fracture pattern of human long bones. These may serve as guidelines for the identification and reconstruction of gunshot trauma in human long bones.

Keywords Forensic anthropology · Human bones · Femur · Humerus · Gunshot · Fracture pattern

Introduction

When dealing with badly preserved cadavers or skeletal human remains, event reconstruction of traumatic cases and determination of the cause of death remain a major challenge

for forensic pathologists and anthropologists. In contrast to fresh or well-preserved cadavers, forensic information in such cases may only be deduced from more resistant tissue such as bone, without further evidence provided by findings on the skin or soft tissue. Although signs of trauma usually

✉ Xavier Jordana
xavier.jordana@uab.cat

✉ Ignasi Galtés
ignasigaltés@gmail.com

¹ Biological Anthropology Unit, Department of Animal Biology, Plant Biology and Ecology, Faculty of Biosciences, Universitat Autònoma de Barcelona, Cerdanyola del Vallès, 08193 Barcelona, Catalonia, Spain

² Forensic Anthropology Unit, Forensic Pathology Service, Catalanian Institute of Legal Medicine and Forensic Science (IMLCFC), Ciutat de La Justícia, Gran Via de Les Corts Catalanes, 111 Edifici G, 08075 Barcelona, Spain

³ Tissue Repair and Regeneration Laboratory (TR2Lab), Institut de Recerca i Innovació en Ciències de La Vida i de La Salut a La Catalunya Central (IrisCC), Ctra. de Roda, 08500 Vic, Barcelona, Spain

⁴ Mossos d'Esquadra, Unitat Central de Balística i Traces Instrumentals, Av. de La Pau, 12, 08206 Sabadell, Barcelona, Spain

⁵ Donor Center Barcelona Tissue Bank (BTB), Hospital Clínic de Barcelona, C/Villarroel 170, Escala 12 Planta 4, 08036 Barcelona, Spain

⁶ Research Group of Biological Anthropology (GREAB), Biological Anthropology Unit, BABVE Department, Universitat Autònoma de Barcelona (UAB), Cerdanyola del Vallès, 08193 Bellaterra, , Catalonia, Spain

persist in bone, reliable forensic conclusions can be considerably complicated, particularly when skeletal remains are shattered or the fractured bones incomplete [1, 2].

Gunshot trauma is widespread not only in armed conflicts, but also in the frame of civil violence [3–6]. Some authors report that at least 50% of the gunshot injuries affect the extremities, often resulting in fractures [7–10]. In this context, the femoral shaft fracture was observed most frequently among ballistic long bone trauma [9]. Despite the frequent occurrence of ballistic long bone trauma, there is only little reliable data in the literature on their fracture characteristics useful for forensic trauma reconstructions.

Studies concerning gunshot trauma have mainly been carried out to analyse cranial fractures [11–13]. There are only a few studies focusing on gunshot trauma in long bones. In 1915, Bland-Sutton described five types of ballistic fractures in human long bones [14]: a projectile impacting a long bone can result in a transverse fracture, completely pierce the diaphysis, stay embedded in the bone, strike the diaphysis and produce a stellate or butterfly pattern, and/or shatter the bone into small fragments. On one hand, this work solely describes the potential fracture type produced by a gunshot without providing details on cortical traits. On the other hand, an actualisation based on current ballistics is required as guns and projectiles have changed since 1915. Since then, however, the majority of the experimental research using human long bones focused on the fracture pathophysiology and risk prediction in relation to different ballistic variables [6, 15–18]. In the 1960s, Huelke et al. used steel spheres with various sizes and velocities to quantify the energy transmitted by the projectiles [16–18]. In the 1980s, Ragsdale and Josselson targeted on cancellous-rich bone areas of distal femurs and proximal tibias, which do not allow the best analysis of cortical bone behaviour [19]. Robens and Küsswetter showed findings in X-rays after a gunshot to the metaphyseal part of the tibias [20]. Also, Coudane et al. studied bone lesions with X-rays after producing gunshot injuries to the limbs of two dead bodies [21]. More recently, Dougherty, Sherman and Bir investigated indirect gunshot impact on diaphyseal femurs and tibia [6]. Bir et al. analysed the fracture risk prediction based on velocity producing both direct and indirect ballistic fractures in human femurs and long bone polyurethane surrogates [15]. Aside from these studies, research on ballistic trauma in human long bones essentially remained descriptive [9, 22–25]. In a more recent review from 2022, Veenstra et al. studied publications providing data on ballistic fractures observed in long bones [26]. The work revealed different types of fractures as a result of gunshot trauma such as linear, oblique, butterfly and comminuted fractures. However, the above-mentioned studies barely provide data on

detailed cortical traits useful for gunshot trauma interpretation, reconstruction and differentiation from other types of trauma.

Further studies on this topic are needed to improve the quality and reliability of the forensic investigation of human long bone trauma. A crucial method to gain further knowledge on detailed ballistic trauma patterns including cortical traits are experimental studies, where the fractures can be reproduced under controlled conditions. In a recent paper, we presented some preliminary data on cortical traits observed in experimentally produced gunshot fractures in human long bones [27]. The purpose of that study was to test whether alternative long bone models such as polyurethane cylinders from Synbone® AG (Switzerland) and female red deer femurs can reproduce the same ballistic fracture patterns. It was revealed that neither the synthetic nor the animal model sufficiently reproduces the human fracture pattern, making these alternative models unsuitable to replace human bones for further fracture investigations.

In the current work, we aim to define a distinctive gunshot fracture pattern in human long bones. Specifically, we propose to reproduce, characterise and discuss the cortical traits related to ballistic long bone trauma and to acquire more knowledge on the underlying fracture mechanism. To this purpose, we have experimentally analysed a broad size of human long bones including femur and humerus. Two different types of long bones were selected to assess if there are considerable differences or if they show similar characteristics indicating that long bones generally produce a similar ballistic fracture pattern. We surrounded the specimens with Clear Ballistics Gel®, a synthetic simulant for soft tissue. In addition, some bones were shot without the gel in order to better visualise the fracture propagation on the high-speed videos. In doing so, we used the opportunity to assess potential differences in the fracture patterns between the specimens shot with and without the soft tissue simulant.

Materials and methods

A total of 29 fresh human healthy bones, 16 femurs and 13 humeri, were used to analyse the fracture type, the fracture propagation and the cortical traits upon gunshot.

Samples and sample preparation

All 29 bones were provided by the Donor Center-Barcelona Tissue Bank, Banc de Sang i Teixits de Catalunya. They were donated from a total of 14 cadavers, 12 males and 2 females. Donor age at death was between 55 and 72 years. All bones were collected with a postmortem time interval of up to 24 h. They were entirely dissected from the limbs and kept in the freezer until further use. Prior to the

experiments, the bones were thawed and the remaining soft tissue was removed up to the periosteum with surgical tools. Subsequently, each bone was macroscopically investigated to exclude pathologies or damage.

To simulate soft tissue, 20 samples, 10 femurs and humeri each, were embedded in ballistic gel. We used a product from the Canadian brand Clear Ballistics, which is supplied as a ready mixed, solid block that requires to be melted at 100 °C for 4 to 5 h before individual application. Clear Ballistics polymer blocks are known for their convenient preparation and exceptional transparency and clearness compared to the standard simulant which is 10% ordnance gelatine [28]. Despite the possibility of reusing this gel, in this study, we consistently employed new gel for the samples. To surround the bones with the gel, we used cylindrical metal moulds with a total diameter of 10 cm. The bones were positioned with the anterior face located 2 cm deep behind the mould's front surface. The liquid gel was poured into the moulds until the bone shaft was entirely surrounded. Subsequently, the gel was left to solidify overnight at room temperature. We observed that air bubbles formed around the bones, which hampered a

clear view on the bone surface. As a consequence, further nine samples, six femurs and three humeri, were shot without gel for a better visualisation of the cracking mechanism on the high-speed recordings. The sample characteristics are summarised in Table 1.

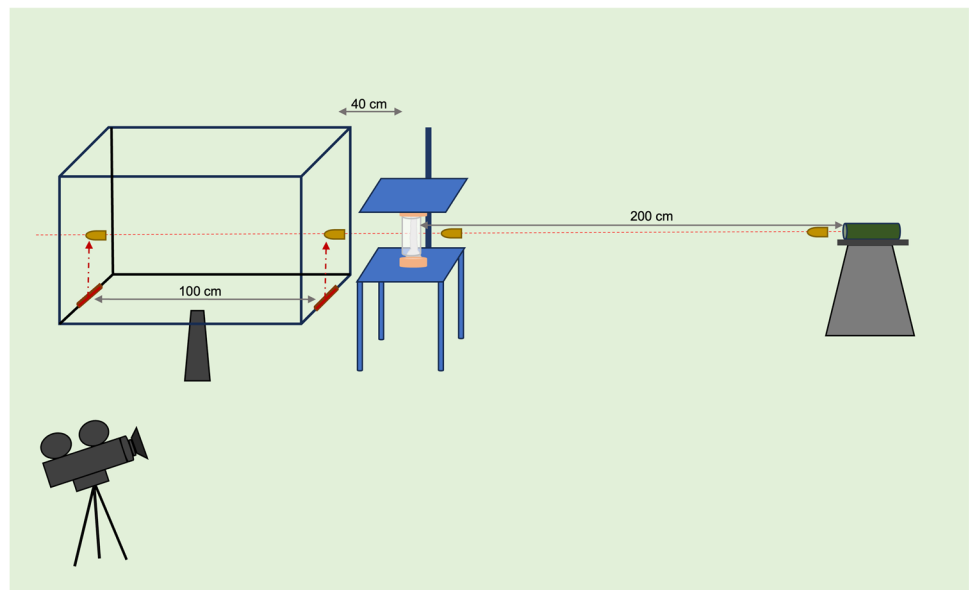
Shooting procedure

All bones were shot under the same condition. Figure 1 illustrates the experimental setup. We securely fixed each specimen upright using a self-constructed stabilisation device. This device was firmly attached to a table. It consisted of a rigid metal plate on the bottom and an adjustable metal plate on the top. The latter could be moved up or down along a steel bar that connected both plates. With the help of two metal cup stabilisers, on each plate one, the bone's epiphyses were held securely. The specimens were placed 2 m before the muzzle of a 9-mm Luger test barrel (Drello Bal 1025 FU-R). While the mechanics of test barrels differ to a certain extent from real firearms, they enable precise, reproducible shots and are commonly employed as a method of experimentation. The bullet impact velocity produced by the test barrel was 360 m/s,

Table 1 Sample group description (*Fem Gel*, =femur with gel; *Fem no Gel*, =femur without gel; *Hum Gel*, humerus with gel; *Hum no Gel*, humerus without gel), revealing the gender, age, bone length, shaft diameter and cortical thickness (mean and standard deviation)

Sample group	<i>N</i>	Male	Female	Age	Bone length (cm)	Shaft diameter (cm)	Cortical thickness (mm)
Fem Gel	10	10	0	62 (5.4)	45.9 (2.8)	2.9 (0.3)	6.2 (0.8)
Fem no Gel	6	2	4	66 (4.9)	44.9 (2.4)	3.0 (0.1)	4.3 (1.5)
Hum Gel	10	10	0	61 (5.0)	32.5 (1.9)	2.1 (0.2)	3.6 (0.8)
Hum no Gel	3	1	2	61 (4.0)	31.0 (0.8)	1.8 (0.5)	3.7 (1.5)

Fig. 1 Experimental setup: test barrel (green) on the right side, fixation table (blue) with metal cup stabilisers (orange) and bone-gel-sample (light grey). Light barrier with two sensors (red) that measure the time the bullet takes from the first to the second sensor. High-speed camera on the bottom left. Distances: 200 cm between muzzle and bone, 40 cm between bone and light barrier, 100 cm between the first and second sensor of the light barrier. The dashed red line indicates the trajectory of the projectile (yellow–brown)



simulating a shot from a handgun. An optical laser was used to define the point of shooting. This was possible in all samples, as the transparency of the ballistic gel allows exact targeting. For the shots, we used a NonTox 9-mm Luger full metal jacket projectile from Sellier & Bellot® ($m=7.98$ g). On each sample, one single projectile was fired in an orthograde manner, whereby the bullet nose struck the middle of the anterior face of the shaft. As the diaphysis has a high corticalis-spongiosa ratio, it allows the best analysis of cortical bone behaviour and hence is more informative than cancellous-rich areas near the epiphysis (Antrag: 43). The exit velocity of the projectile upon impact was measured using a light barrier (Drello LS 11–03) with a computerised system (Drello VC 4043–09). The performance was recorded with a high-speed camera (Phantom V2012).

Sample assessment

The fragments of each shot specimen were collected and cleaned prior to analysis. In doing so, the bones were cooked at 100 °C for 2 to 5 h in a water detergent solution consisting of 5 L of plain water and 1 cup of commercial degreasing detergent [29]. Subsequently, the bones were scrubbed smoothly to clear away the periosteum. After the bones were left to dry, the fragments of each sample were reassembled using a superglue. This allowed us to better visualise the fracture patterns. The fractures were examined macroscopically. The fracture type was determined by its appearance on the impact side. The cortical traits were classified into entrance, exit and general features. For quantitative analyses, we used a calliper to measure the maximal longitudinal fracture extent and the horizontal and vertical diameter of the projectile's entrance and exit hole. The projectiles' post-impact velocity was used to calculate the kinetic energy lost in each bone ($Ke=0.5 mv^2$).

After the collection of all data, the ballistic fracture patterns were defined. In doing so, we grouped the samples into femurs with and without gel and humeri with and without gel. Logistic regression and two-way ANOVA (Tukey post hoc tests) were performed to statistically test the effect of ballistic gel and the type of bone (femur and humerus) in the occurrence of fracture characteristics. The significance level was set at 0.05. A multiple correspondence analysis was done to explore correlations between the fracture traits (qualitative and quantitative), experimental groups (type of bone and use of gel) and bone properties (length, shaft diameter and cortical thickness).

Results

Upon gunshot, all samples exhibited comminuted fracture accompanied by severe fragmentation into small bone chips. Nevertheless, assembling the bigger fragments allowed a

more comprehensive fracture reconstruction and a sound macro-morphological assessment. Tables 2, 3 and 4 and Figs. 2, 3 and 4 present the qualitative cortical traits classified into entrance, exit and general features that characterise the ballistic fracture pattern in human long bones. In total, 24 qualitative and 6 quantitative variables were determined.

The entrance fracture pattern

Table 5 shows the occurrence of the cortical entrance traits in the sample groups. Figures 2 and 3 illustrate the entrance fracture with the detailed cortical traits. In each case, the entrance fracture featured a round entry hole with various radiating and concentric fractures. On the impact side, this visually resulted in a stellate pattern. Longitudinal concentric fractures around the entry hole were observed in all samples. They could typically be seen on the lateral shaft aspect. Transversal concentric fractures were less frequent. In the gel samples, they occurred in none of the femurs (0%) and in three out of ten humeri (30%). In the samples without gel, they occurred in two out of six femurs (33%) and in one out of three humeri (33%). Differences between sample groups were not statistically significant.

V-shape, ring defect, internal beveling and wing piece were featured by all samples. A lateral notch was found in all femurs with and without gel (100% each), in all humeri without gel (100%) and in nine out of ten humeri with gel (90%). There were no significant differences between the sample groups. Tip fragmentation was featured in all femurs and humeri without gel (100% each) and in nine out of ten femurs and humeri with gel, respectively (90% each). The difference between the samples, however, was not statistically significant. Wing flake was most common in gel femurs with seven out of ten positive cases (70%). In contrast, they were not found in any of the femurs without gel (0%). In gel humeri, they occurred in five out of ten cases (50%), and in humeri without gel in one out of three cases (33%). Logistic regression revealed a significant correlation between the presence of gel and the occurrence of wing flakes (p value = 0.031, odds ratio = 12.5). Wing flake defect was featured by all femurs with gel (100%) and three out of six femurs without gel (50%). In humeri, the trait was found in five out of ten with gel (50%) and in two out of three without gel (67%). Logistic regression did not reveal a significant difference, but yet showed that the occurrence of a wing flake defect is close to significantly greater in femurs than humeri (p value = 0.081, odds ratio = 0.19).

As quantitative entrance variables, we measured the vertical and horizontal entry hole diameter (Table 6, Fig. 5). The latter, however, could not be evaluated for all samples as a complete entry hole reconstruction was not always possible. The mean vertical entry hole diameter was the largest in femurs, both with (10.1 ± 1.0 mm) and without gel (10.1 ± 0.5 mm). In humeri with gel, it was 9.8 ± 0.7 mm,

Table 2 Trait definition at the entrance fracture

Round entry hole	The projectile's initial entry defect appearing visually round
Radiating fracture	Longitudinal, transversal or oblique fractures that radiate away from the entry hole
Concentric fracture	Curvilinear fractures facing with their concave aspect towards the entry hole. They were divided into transversal or longitudinal ones. The first occurs proximal/distal of the entry hole, the second on the sides of the entry hole
V-shape	Describes the shape of the bone proximal/distal to the entry hole. The tip of the v-shape points towards the bullet entry. The margins of the v-shape are built by oblique fracture lines
Tip fragmentation	A superficial, external loss of cortical fragment(s) at the tip of the bone around the entry hole. It only appears proximal/distal of the bullet entry. Typically, chiselled edges indicate a sharply defined transition to the intact cortical bone. In case oblique fractures separate the bone, tip fragmentation on bone parts next to each other creates the image of a stepped circular margin around the bullet entry
Ring defect	A circular or partial circular loss of superficial cortical bone on the entry hole's margin. Its presentation reminds of an abrasion ring. It can be interrupted by other entrance traits such as tip fragmentation
Wing flake	A loose trapezoidal flake of cortical bone resembling spread wings. The aspect facing the entry hole features part of the ring defect. In contrast to tip fragmentation, it comes from the lateral aspect(s) of the entry hole. It may be broken and thus incomplete
Wing flake defect	The superficial cortical defect on the lateral aspect(s) of the entry hole that is produced when the wing flake breaks out
Internal beveling	A funnel shape in the cortical wall with a larger extent on the internal side
Wing piece	A bone fragment originating from the lateral shaft aspect(s). Its shape is similar to the wing flake, but it is usually much bigger, and most importantly, it affects the hole cortical wall; only the extremes run out superficially. The aspect facing the entry hole may contain part of the ring defect or a wing flake defect. A wing piece can be entire, but also broken into two or more fragments. Less frequently, they may be still attached on one side of the shaft
Lateral notch	As the wing piece's extremes run out superficially, they leave behind a corresponding cortical defect on the lateral shaft aspect. On this fracture surface, there is a prominent notch visible

Table 3 Trait definition at the exit fracture

Square exit hole	The projectile's exit defect appears visually edgy or square
Radiating fracture	Transversal, longitudinal or oblique fractures that radiate away from the exit hole
Concentric fracture	Curvilinear fractures facing with their concave aspect towards the exit hole. They were divided into transversal or longitudinal ones. The first occurs proximal/distal of the exit hole, the second on the sides of the exit hole
Layered breakage	Is a layered pattern visible on the fracture surface
External beveling	A funnel shape in the cortical wall with a larger extent on the external side
Stepped breakout	A sequence of multiple transversal concentric fractures on the posterior shaft aspect resulting in a stepped breakout of fragments with similar shapes

Table 4 General trait definition

Plastic deformation	Is the persistent deformation of bone
Marginal chipping	Tiny, superficial cortical defects on the fracture margin
Fx surface scaling	Tiny cortical scaling on the fracture surface

and in humeri without gel the smallest with 9.2 ± 0.3 mm. There was no significant difference between the sample groups. The largest mean horizontal diameter was established for femurs with gel (10.1 ± 0.7 mm). In contrast, the smallest mean horizontal diameter was found in femurs without gel (8.3 ± 0.9 mm). In humeri with gel, it was 9.8 ± 0.9 mm. In humeri without gel, only one sample could be evaluated revealing a horizontal diameter of 9.5 mm. Two-way ANOVA showed significant differences in the size of the horizontal entry hole diameter between samples with and without gel (p value = 0.002, $\eta^2 = 0.39$).

The exit fracture pattern

Table 5 shows the occurrence of all cortical exit traits in the sample groups. In all samples, we observed an exit hole with various radiating and concentric fractures. The transversal concentric fractures were present in all femurs and humeri with gel (100% each), in all humeri without gel (100%) and in five out of six femurs without gel (83%). There were no significant differences between the sample groups. Longitudinal concentric fractures were present in seven out of ten femurs and six out of ten humeri with gel (70% and 60% respectively). In

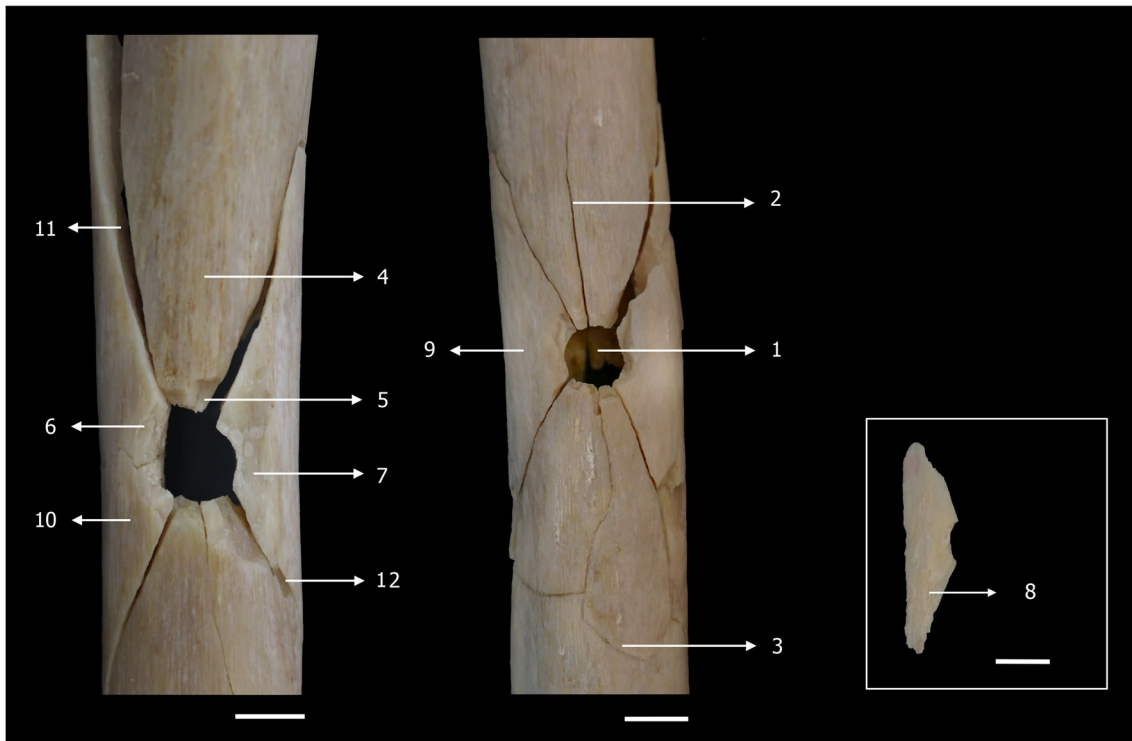


Fig. 2 Anterior view of two shot femurs (white bar=1 cm). Entrance traits: round entry hole (1), radiating fracture (2), transversal concentric fracture (3), v-shape (4), tip fragmentation (5), ring defect (6),

wing flake defect (7), wing flake (8), wing piece (9), transversally broken wing piece (10). General cortical traits: plastic deformation (11), marginal chipping (12)

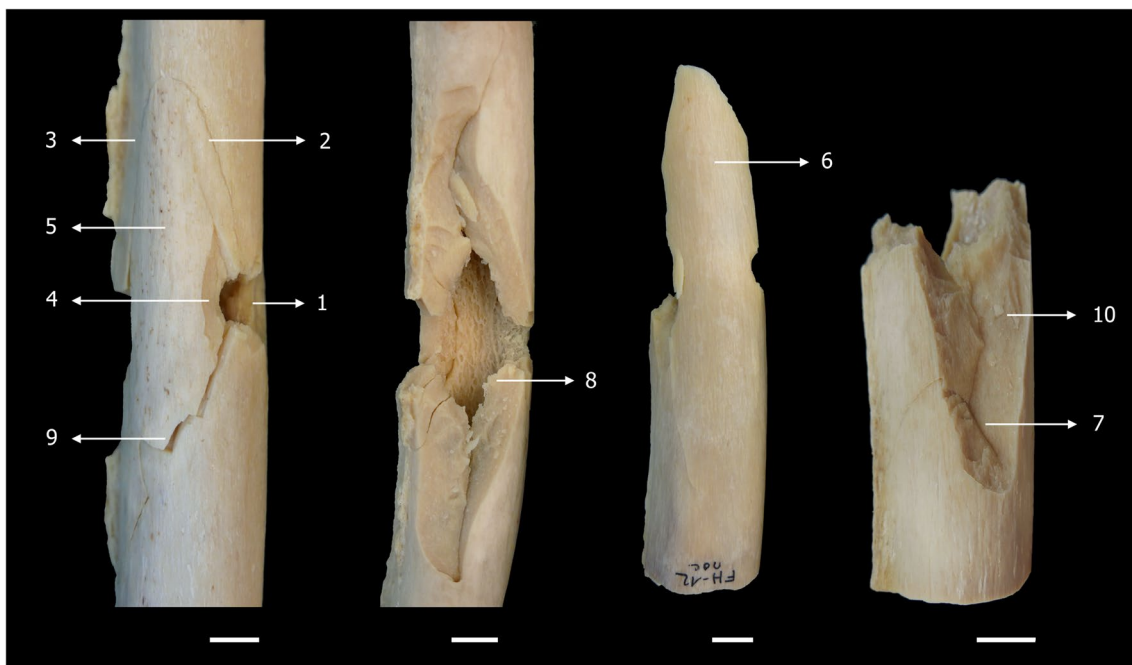
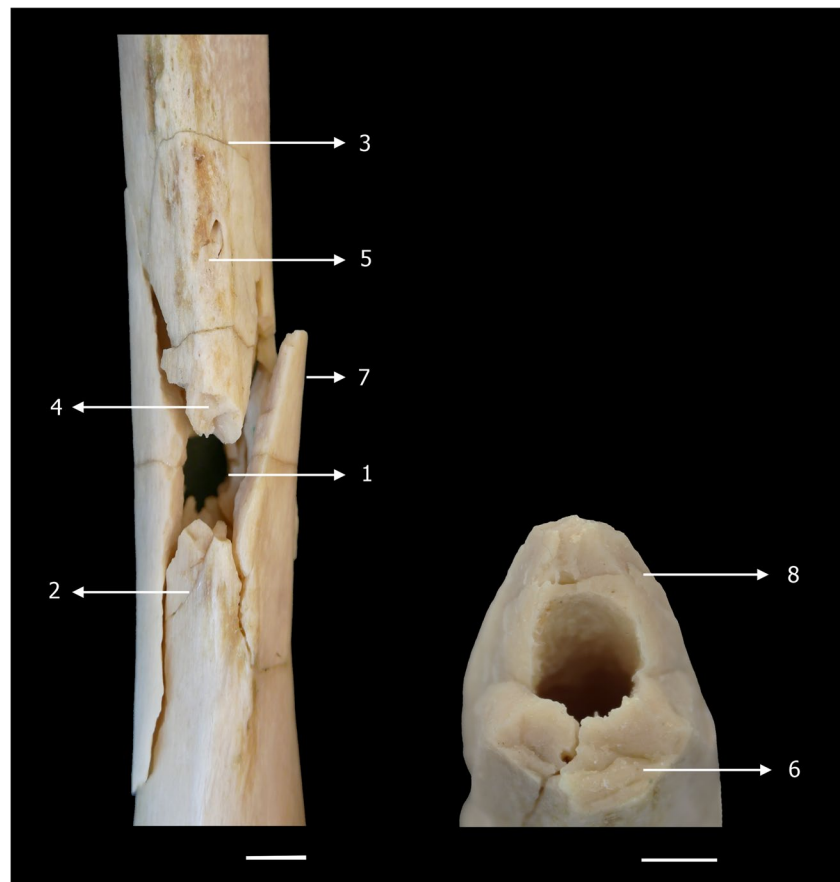


Fig. 3 Lateral view of four shot femurs (white bar=1 cm). Entrance traits: round entry hole (1), radiating fracture (2), longitudinal concentric fracture (3), wing flake defect (4), wing piece (5), wing piece

attached to the shaft (6), lateral notch (7), internal beveling (8). General cortical traits: plastic deformation (9), Fx surface scaling (10)

Fig. 4 Posterior view and superior view of two shot femurs (white bar = 1 cm). Exit traits: square exit hole (1), radiating fracture (2), transversal concentric fracture (3), external beveling (4), stepped breakout (5), layered breakage (6). General cortical traits: plastic deformation (7), Fx surface scaling (8)



the samples without gel, they were present in three out of six femurs (50%) and in none of the humeri (0%). There were no significant differences between the sample groups.

A square exit hole was found in all humeri with and without gel (100% each). In femurs, it was found in nine out of ten with gel (90%) and in five out of six without gel (83%). There were no significant differences between the sample groups. The two femurs, one with and one without gel, which did not have a square exit hole, presented a round exit hole. Stepped breakout was found in six out of ten femurs with gel (60%) and five out of six femurs without gel (83%). In humeri, it was less common with an occurrence of two out of ten with gel (20%) and a complete absence in the ones without gel (0%). Logistic regression revealed that the occurrence of stepped breakout is significantly greater in femurs than humeri (p value = 0.009, odds ratio = 0.08). Layered breakage occurred in nine out of ten femurs and eight out of ten humeri with gel (90% and 80% respectively). In the samples without gel, it occurred in four out of six femurs (67%) and in one out of three humeri (33%). The logistic regression showed no significant, but yet a close correlation between the presence of gel and layered breakage (p value = 0.075, odds ratio = 5.9). External beveling was detected in all femurs with and without gel (100% each) and

in all humeri with gel (100%), but only in one out of three without gel (33%). However, statistically significant differences between sample groups were not found.

Quantitatively, the vertical and horizontal exit hole diameters were evaluated; however, the consistent measurement was hampered as the exit hole could not always be entirely reconstructed (Table 6 and Fig. 5). Notably, it was not possible with any of the no gel humeri. The mean vertical exit hole diameter was the largest in humeri with gel (21.6 ± 9.6 mm). In the femurs with gel, it was 18.2 ± 6.3 mm, and in femurs without gel the smallest with 15.0 ± 6.9 mm. There were no significant differences between the groups. The mean horizontal exit hole diameter was the largest in femurs with gel (10.5 ± 1.8 mm). In the humeri with gel, it was 9.5 ± 1.7 mm, and in femurs without gel the smallest with 7.9 ± 2.6 mm. Two-way ANOVA showed that the size of the horizontal exit hole diameter was significantly larger in samples with gel than without gel (p value = 0.026, $\eta^2 = 0.234$).

The general fracture characteristics

Some general cortical traits could be detected without a relation to the entrance or exit fracture. All samples showed plastic deformation, marginal chipping and fracture surface

Table 5 Analysed cortical traits divided into entrance, exit and general traits (**p* value < 0.05, ***p* value < 0.01)

	Femur gel		Femur no gel		Humerus gel		Humerus no gel	
	<i>N</i>		<i>N</i>		<i>N</i>		<i>N</i>	
Entrance traits								
Round hole	10	100%	6	100%	10	100%	3	100%
V-shape	10	100%	6	100%	10	100%	3	100%
Tip fragmentation	9	90%	6	100%	9	90%	3	100%
Ring defect	10	100%	6	100%	10	100%	3	100%
Wing flake	7	70%	0	0%	5	50%	1	33%
Wing flake defect	10	100%	3	50%	5	50%	2	67%
Internal beveling	10	100%	6	100%	10	100%	3	100%
Wing piece	10	100%	6	100%	10	100%	3	100%
Lateral notch	10	100%	6	100%	9	90%	3	100%
Radiating fracture	10	100%	6	100%	10	100%	3	100%
Concentric fracture	10	100%	6	100%	10	100%	3	100%
Transversal	0	0%	2	33%	3	30%	1	33%
Longitudinal	10	100%	6	100%	10	100%	3	100%
Exit traits								
Square hole	9	90%	5	83%	10	100%	3	100%
External beveling	10	100%	6	100%	10	100%	1	33%
Layered breakage	9	90%	4	67%	8	80%	1	33%
Stepped breakout	6	60%	5	83%	2	20%	0	0%
Radiating fracture	10	100%	6	100%	10	100%	3	100%
Concentric fracture	10	100%	6	100%	10	100%	3	100%
Transversal	10	100%	5	83%	10	100%	3	100%
Longitudinal	7	70%	3	50%	6	60%	0	0%
General traits								
Plastic deformation	10	100%	6	100%	10	100%	3	100%
Marginal chipping	10	100%	6	100%	10	100%	3	100%
Fx surface scaling	10	100%	6	100%	10	100%	3	100%

scaling (Table 5). As shown in Table 6 and Fig. 5, the mean fracture extent was the largest in femurs with gel (14.9 ± 3.3 cm), followed by femurs without gel (14.3 ± 2.6). In humeri with gel, it was 9.2 ± 1.7 cm, and in humeri without gel the smallest with 8.3 ± 1.9 cm. Two-way ANOVA showed that the fracture extent was significantly larger in femurs than in humeri (*p* value < 0.001, $\eta^2 = 0.58$).

Video analysis

Figure 6 shows a sequence of images from two high-speed videos. Despite the clarity and transparency of the Clear Ballistics Gel®, the densely arranged air bubbles around the bone significantly hindered the analysis of the fracture propagation in the recordings. In this regard, to assess the fracture propagation during gunshot, only the samples without gel allowed an accurate analysis. On the high-speed videos of these samples, we saw that the bullet penetrates the anterior and posterior wall of the shaft producing a direct entrance

and exit fracture, respectively. As a further result, we found when the bullet penetrates the anterior wall, radiating fractures initiate on the front side. On the lateral aspect, concentric fractures develop just before the radiating fractures are fully extended. With fracture progression, the radiating and concentric fractures merge. In doing so, the lateral wing piece is formed and eventually blown out laterally as a consequence of the blast effect when the bullet penetrates the shaft.

The bullet's energy lost upon impact

The projectile's exit velocity was measured to calculate the energy lost upon impact (Table 6 and Fig. 5). However, the measurements were not successful in all samples due to interferences with the light barrier caused by bullet fragments and in case of no gel samples also bone fragments. The greatest mean energy loss was observed in femurs with gel (348.6 ± 69.7 J), whereas in femurs without gel, it was only 264.4 ± 99.1 J. In humeri with gel, it

Table 6 Descriptive statistics of the analysed quantitative (*VD*, vertical diameter; *HD*, horizontal diameter; *Fem Gel*, femur with gel; *Fem no Gel*, femur without gel; *Hum Gel*, humerus with gel; *Hum no Gel*, humerus without gel)

	Group	<i>N</i>	Mean	SD	Min	Max
Entry hole <i>VD</i> (mm)	Fem Gel	10	10.1	1.0	9.0	11.5
	Fem no Gel	6	10.1	0.5	9.5	11.0
	Hum Gel	10	9.8	0.7	9.0	11.0
	Hum no Gel	3	9.2	0.3	9.0	9.5
Entry hole <i>HD</i> (mm)	Fem Gel	10	10.1	0.7	9.0	11.0
	Fem no Gel	4	8.3	0.9	7.5	9.0
	Hum Gel	7	9.8	0.9	9.0	11.0
	Hum no Gel	1	9.5			
Exit hole <i>VD</i> (mm)	Fem Gel	10	18.2	6.3	12.5	29.0
	Fem no Gel	6	15.0	6.9	9.0	27.0
	Hum Gel	10	21.6	9.6	13.0	40.5
	Hum no Gel	0				
Exit hole <i>HD</i> (mm)	Fem Gel	10	10.5	1.8	7.5	13.0
	Fem no Gel	5	7.9	2.6	4.0	11.0
	Hum Gel	7	9.5	1.7	8.0	12.5
	Hum no Gel	0				
Fracture extent (cm)	Fem Gel	10	14.9	3.3	11.2	21.5
	Fem no Gel	6	14.3	2.6	11.2	16.6
	Hum Gel	10	9.2	1.7	6.5	12.0
	Hum no Gel	3	8.3	1.9	6.2	9.8
Energy loss (J)	Fem Gel	6	348.6	69.7	237.4	444.6
	Fem no Gel	4	264.4	99.1	157.5	375.1
	Hum Gel	8	261.1	61.3	193.8	379.2
	Hum no Gel	1	258.8			

was 261.1 ± 61.3 J), and in humeri without gel, we could only calculate the energy loss in one out of three samples, which was 258.8 J. Two-way ANOVA showed that the higher energy loss in gel femurs compared to the energy loss in gel humeri was close to significant (p value = 0.059, $\eta^2 = 0.206$).

Multiple correspondence analysis

A multiple correspondence analysis was done in order to observe correlations among fracture characteristics, bone properties and sample groups (Fig. 7 and Table 7).

Dimension 1 (21% of the variance) shows that gel was especially important in the presence of both wing flake and wing flake defect, as well as the absence of transversal concentric fractures at the bullet entrance. To a lesser extent, gel also had an influence on the presence of external beveling. In contrast, the type of bone (humerus or femur) did not show a significant correlation with the fracture characteristics. Yet, a correlation between bone properties such as cortical thickness and shaft diameter with the occurrence of wing flake, wing flake defect, external beveling and a larger horizontal entry hole diameter has been found.

Dimension 2 (15% of the variance) shows a correlation between a squared exit hole and a higher vertical exit hole

diameter, as well as a correlation between absent stepped breakout and absent transversal concentric fractures around the exit hole. The latter was expected, as the stepped breakout is formed by a repetition of transversal concentric fractures.

Ultimately, dimension 3 (14% of the variance) correlates bone properties such as the shaft diameter and bone length with fracture characteristics such as a larger vertical entry hole diameter, a not squared exit hole and a greater occurrence of longitudinal concentric fractures at the exit.

Discussion

In good preserved cadavers, skin and soft tissue injuries typically show characteristic features allowing conclusions on the applied mechanical force such as gunshot, blunt force, sharp force or other impacts [30]. In gunshot trauma, the ballistic characteristics of entrance and exit skin wounds are widely accepted and applied in routine forensic investigations, while less precise morphological information is given for bones. The interpretation and reconstruction of ballistic bone trauma is particularly challenging when dealing with long bones as conclusive

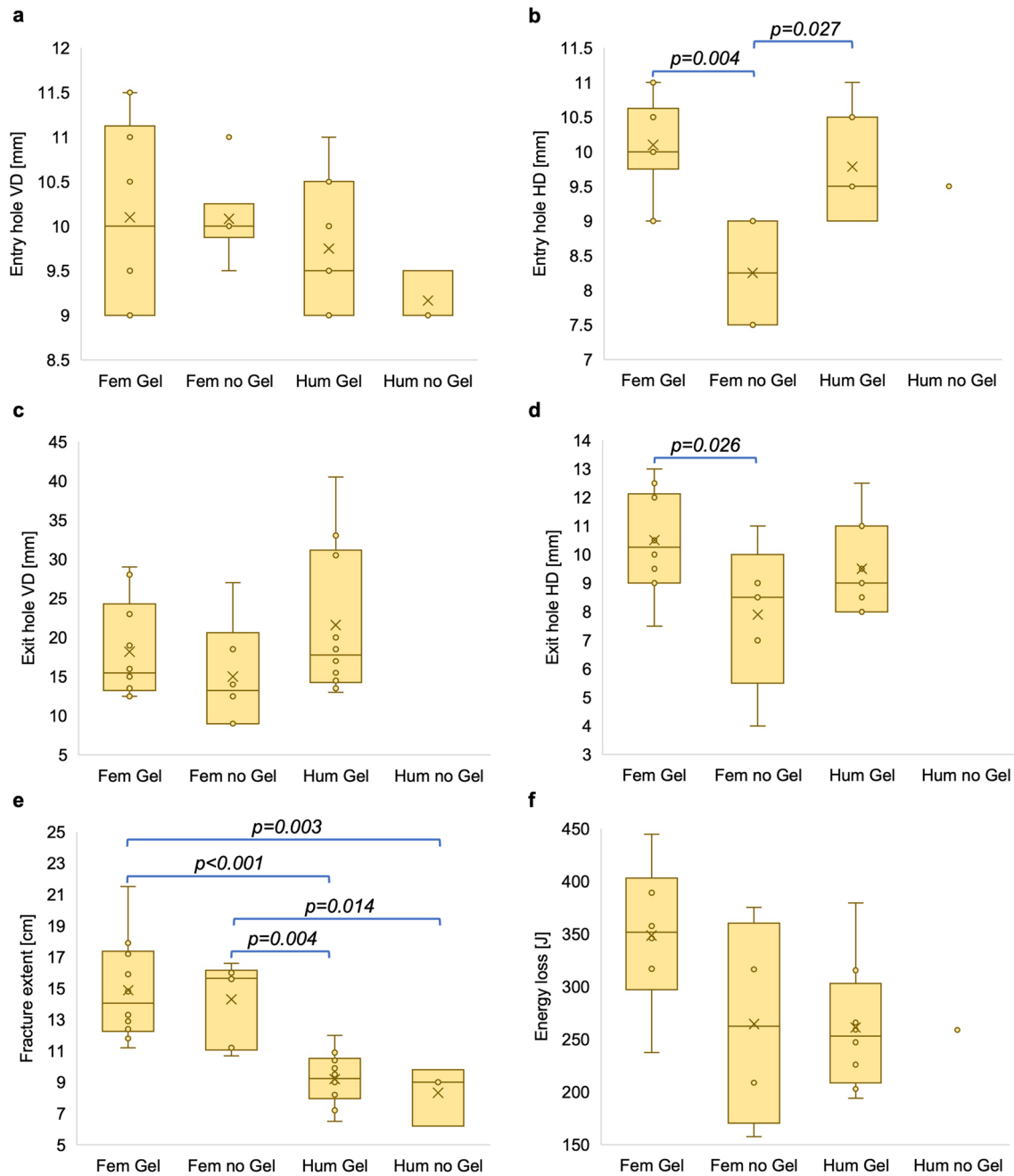


Fig. 5 Box plots representing the **a** vertical entry hole diameter, **b** horizontal entry hole diameter, **c** vertical exit hole diameter and **d** horizontal exit hole diameter, **e** fracture extent and **f** projectiles' energy lost upon impact (VD=vertical diameter, HD=horizontal

diameter, Fem Gel=femur with gel, Fem no Gel=femur without gel, Hum Gel=humeral with gel, Hum no Gel=humeral without gel) (significant p values for the pairwise comparison)

data is scarce. To resolve such uncertainty, realistic experiments are of great importance. As we revealed in a previous study, the selection of alternative models is problematic because animal bones and bone surrogates are too dissimilar to human bones [27]. In this study, we shot ten femurs and ten humeri with ballistic gel and six femurs and three humeri without ballistic gel. We

examined in a comprehensive way the macroscopic characteristics in order to provide supportive guidelines for the ballistic trauma interpretation. Consistently, a comminuted fracture was reproduced, which according to the literature is the most common type of diaphyseal gunshot trauma [26]. In line with the postulation that particularly the bullet impact region is of high conclusive value [27,

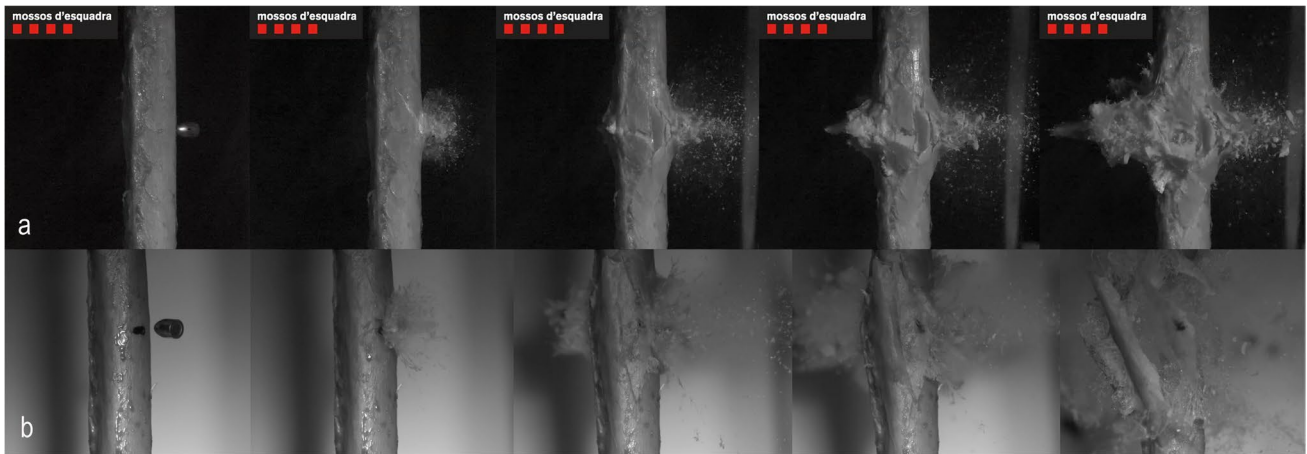


Fig. 6 Sequence of images from high-speed videos capturing the shot of two femurs without gel, from the **a** lateral-posterior perspective showing the bullet entry and exit and the blast effect, and **b** lateral-

anterior perspective showing the formation of first radiating and then concentric fractures at the entrance and the blast out of the wing piece

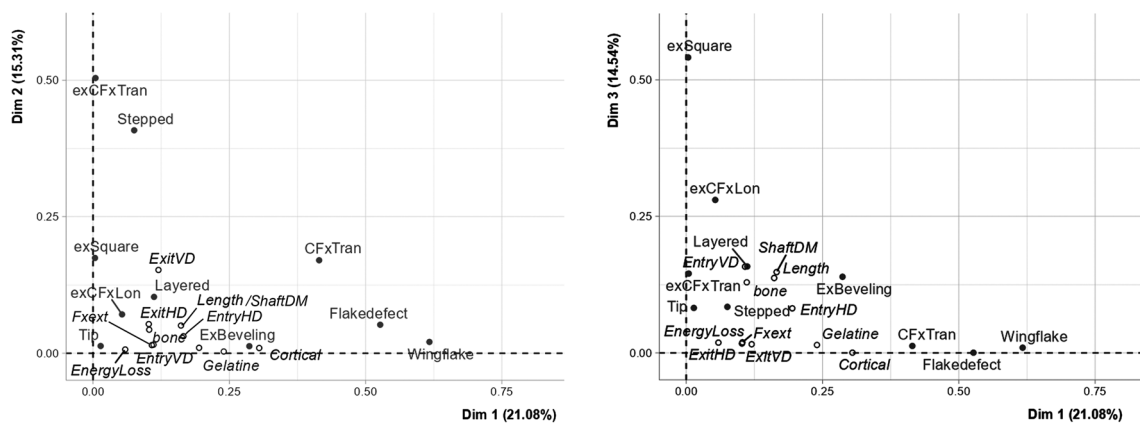


Fig. 7 Multiple correspondence analysis showing the three first dimensions. Representation of the variables: exCFxTran=transversal concentric fracture of the exit, Stepped=stepped breakout, exSquare=squared exit hole, exCFxLon=longitudinal concentric fracture of the exit, Fxext=fracture extent, Tip=tip fragmentation, ExitVD=vertical exit hole diameter, Layered=layered breakage, ExitHD=horizontal exit hole diameter, EntryVD=vertical entry

hole diameter, EntryHD=horizontal entry hole diameter, ExBeveling=external beveling of the exit hole, CFxTran=transversal concentric fracture of the entry, Flakedefect=wing flake defect, Wingflake=wing flake, EnergyLoss=bullet’s energy loss, bone=type of bone (femur or humerus), Gel=ballistic gel, Length=bone length, ShaftDM=shaft diameter, Cortical=cortical thickness

31], the entrance fracture provided more characteristics than the exit fracture. Figure 8 illustrates the scheme of paradigmatic diaphyseal gunshot fracture resulting from the gunshot scenario tested in this study. In all sample groups, we found a similar ballistic fracture pattern. However, the occurrence values of some traits differed between the groups. The results support the relevance of using a soft tissue simulant, but are not entirely in line with the assumption that the biomechanics behind gunshot trauma are similar in all tubular bones [32]. A detailed discussion of the traits and their correlation to ballistic gel and bone properties is provided in the following paragraphs.

Entrance fracture and fracture type

In the literature, the fracture type in ballistic long bone trauma is commonly classified as a stellate pattern, indicating that multiple fractures radiate from the entry hole [14, 25, 33, 34]. Other authors refer to butterfly fractures [14, 18, 34, 35]. Yet, there is a controversy in using this term as it implies a different fracture mechanic occurring classically in blunt force trauma [36]. There, a real butterfly fracture is thought to initiate on the tension side of the shaft, which is opposite to the impact side [37, 38]. In contrast, ballistic fractures initiate at the impact side. Hence, some authors also use the term false butterfly fracture to describe this reverse phenomenon [37,

Table 7 Description of the axes of the multiple correspondence analysis. Significant correlations of the traits with the three first dimensions are shown. Category: (+) trait presence or (-) trait absence of the qualitative traits. Representation of the variables: *Wingflake*, wing flake; *Flakedefect*, wing flake defect; *CFxTran*, transversal concentric fracture of the entry; *Cortical*, cortical thickness; *ExBeveling*, external beveling of the exit hole; *Gel*, ballistic gel; *EntryHD*, horizontal entry hole diameter; *ShaftDM*, shaft diameter; *Length*, bone length; *exCFxTran*, transversal concentric fracture of the exit; *Stepped*, stepped breakout; *exSquare*, squared exit hole; *ExitVD*, vertical exit hole diameter; *exCFxLon*, longitudinal concentric fracture of the exit; *EntryVD*, vertical entry hole diameter; *Layered*, layered breakage

Percentage of the variance	Trait	Category	R ²	p value
Dim 1 (21.08%)	Wingflake	+	0.61	0.001
	Flakedefect	+	0.52	0.001
	CFxTran	-	0.41	0.001
	Cortical		0.30	0.001
	ExBeveling	+	0.28	0.002
	Gel	+	0.23	0.007
	EntryHD		0.19	0.01
	ShaftDM		0.17	0.02
	Length		0.16	0.03
Dim 2 (15.31%)	exCFxTran	-	0.50	0.001
	Stepped	-	0.41	0.001
	exSquare	+	0.17	0.02
	CFxTran	-	0.17	0.02
	ExitVD		0.15	0.03
Dim 3 (14.54%)	exSquare	-	0.54	0.001
	exCFxLon	+	0.28	0.001
	EntryVD		0.16	0.03
	Layered	-	0.16	0.03
	ShaftDM		0.14	0.03
	exCFxTran	-	0.14	0.04
	ExBeveling	+	0.14	0.04
Length		0.13	0.04	

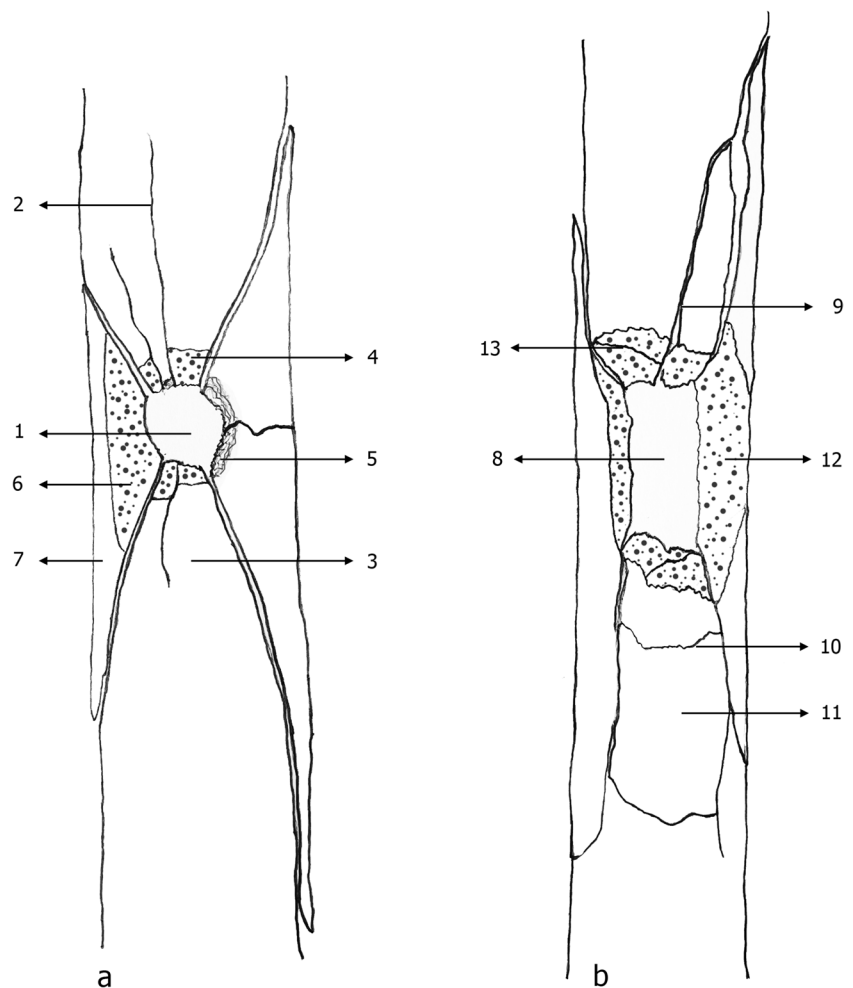
39]. Lower gunshot velocities have also been linked to other patterns such as spiral, oblique or bore-hole fractures [14, 20, 24, 34, 39]. In our study, the impact side revealed an entry hole with radiating and concentric fractures, similar to the findings by Martrille and Symes and Smith et al. [13, 25]. As these fracture components also appear in skulls, Smith et al. claimed that long bone and cranial gunshot trauma is comparable. In general, the formation of radiating and concentric heaving fractures is strongly related to large amounts of kinetic energy [1, 13, 25, 40]. Principally, radiating fractures without concentric ones can occur when they are sufficient to relieve the pressure [41]. In contrast, concentric fractures do not occur solely. In cranial gunshot trauma, they were related to the increased intracranial pressure and blast effect upon bullet penetration [41]. Long bones can also be considered hollow organs with a solid wall. Thus, increased pressure in the shaft and cavity formation are thought to be

part of the ballistic fracture mechanism [42]. In cranial gunshot trauma, radiating and concentric fractures are usually visible at the impact side [1]. Authors described the concentric form after the radiating ones and end perpendicularly at them [1, 11]. The fracture image reminds of a spiderweb and thus is referred to as a spiderweb-like pattern [1]. In long bones, we saw concentric fractures are often not visible on the frontal view since they appear mostly lateral on the shaft. Hence, they are less commonly transversal ones on the anterior aspect. Soft tissue simulant was even revealed to reduce their appearance. In addition, we observed the concentric fractures typically merge with the radiating ones instead of ending perpendicularly at them. As a consequence, the definition of a classical spiderweb-like pattern may not be entirely accurate for ballistic long bone trauma. In summary, although the classification is not that trivial, we consider the stellate pattern to be the most suitable to describe the fracture type revealed in our study.

Beyond the fracture type, radiating and concentric fractures also formed distinctive cortical entry traits. The *v-shape* is formed by radiating fractures, defines the anterior silhouette of the shaft and indicates the bullet impact with its tip. We recognised this characteristic in a work from Baraybar and Gasior [43], who analysed long bone fractures of real gunshot victims. The *wing piece* is formed by the fusion of radiating and concentric fractures. It is mostly detached from the shaft, but easy to recognise among other fragments due to its characteristic shape. Martrille and Symes described it as a pie-shaped fragment that can be confused with the wings of a butterfly fracture [25]. On our high-speed videos, we saw the wing piece was laterally blasted off the shaft. This is in line with Di Maio, who explained when a bullet penetrates a bone, it creates a temporary cavity causing the bone fragments to be propelled laterally [31]. After the wing piece breaks out, a prominent *lateral notch* can be seen on the shaft.

Focusing on the entry hole, we consistently found a round shape as well reported in perpendicular impacts [25, 41]. On the interior surface, all specimens exhibited *internal beveling*, a cone shape due to bone shards knocked off in the bullet's flight direction [11, 31, 44–47]. The entry hole size did not precisely reflect the bullet diameter. Comparable findings exist for cranial gunshot wounds, where it is reported that an exact calibre estimation is not possible [48–50]. In the majority of our cases, both the vertical and horizontal diameters were slightly larger than the bullet diameter. This may be attributed to a loss of cortical bone around the entrance hole, mainly due to a ring defect as discussed below. In addition, our results revealed the entry hole is bigger in larger bones. Moreover, the horizontal entry hole diameter was revealed to be bigger when soft tissue simulant was present. Interestingly, in femurs without gel, we even found a smaller horizontal entry hole than bullet diameter.

Fig. 8 Scheme of a paradigmatic entrance and exit fracture in a femur upon perpendicular impact of a 9-mm FMJ bullet shot at a handgun speed from a distance of 2 m: **a** anterior shaft aspect illustrating the following entrance traits: round entry hole (1), radiating fracture (2), v-shape (3), tip fragmentation (4), ring defect (5), wing flake defect (6), wing piece (7); **b** posterior shaft aspect illustrating the following exit traits: square exit hole (8), radiating fracture (9), transversal concentric fracture (10), stepped breakout (11), external beveling (12), layered breakage (13)



In the literature, a smaller entry hole than a bullet diameter is described as possible but less common [41]. Some authors explained this phenomenon by the elasticity of fresh bone [51, 52]. In general, our results support the evidence that an exact representation of the bullet size cannot be expected as bone is a material that can deform under force [40].

Around the entry hole, we observed distinguishable external cortical lesions. Hereby, a proper trait discrimination ensures to not confound them with external beveling of exit holes. A *ring defect* is a very superficial cortical loss at the edge of the entrance wound. Similar findings have been observed in cranial gunshots [31, 47, 53, 54]. *Tip fragmentation* is more irregular and is the consequence of bone chips that have been pushed off proximal and distal of the bullet entry. A *wing flake defect* occurs on the lateral aspects of the entry hole after a *wing flake* is pushed off upon bullet impact. Despite the link between both traits, wing flakes could not be found in all cases with wing flake defect. A potential explanation is that flakes shatter and are not recognisable anymore. In the recovery of real skeletonised remains, it is conceivable that wing flakes are difficult to find as they are small and can get easily lost. Our results indicate that cortical thickness

and shaft diameter as well as soft tissue have an important influence on the presence of wing flakes. General bone chipping and delamination around the entry hole have also been reported [25]; however, there is no specific terminology that helps the reconstruction and identification of the entry hole. Although perpendicular bullet impacts in skulls usually result in smooth or sharp-edged entry holes [13, 31, 42], external bone chipping has been observed too [47, 53–56]. Regarding the trauma mechanism, bone chipping in general has been linked to increasing kinetic energy [37]. In gunshot trauma, authors have discussed bone chipping due to gases in contact shots [53], the projectile's twisting force [53, 55], a backward explosion after released kinetic energy [54, 56] and a temporary cavity-induced blowback [56].

Exit fracture

In the literature, authors reported on missing exit defects, which they explain by the fact that entry fractures cause the opposite shaft side to break before the bullet impacts there [13, 25]. In our study, all samples revealed an exit hole with

radiating and concentric fractures. Nevertheless, we saw that entry-associated fractures predominantly extended laterally towards the posterior shaft aspect. This clearly influenced the shape of the exit fracture respecting the Puppe rule [57], and may explain why longitudinal concentric fractures (on the lateral shaft aspects) were less common than transversal ones.

In line with other authors, we found the exit wound was quite destructive, characterised by a substantial fragmentation resulting predominantly in a large square hole, not to be confused with the small round entry hole [36, 39, 58]. An explanation may be considered the structural damage of the bullet after entering the shaft, such as deformed circular shape and increased contact surface, leading to a high energy transmission and tissue damage [36]. Our results further showed that square exit holes correlate with a larger vertical exit hole diameter. The less common round exit hole is smaller, linked to longitudinal concentric fractures, and more likely to be found when both bone length and shaft diameter increase. The horizontal exit hole diameter, however, was shown to be larger with the presence of the soft tissue simulant.

Furthermore, we revealed additional distinctive cortical traits to identify the bullet exit. *External beveling*, as it is well known from cranial exit wounds [47, 59], was also present in our long bones. Our results indicate that it correlates with the presence of the soft tissue, cortical thickness, bone length and shaft diameter. *Layered breakage* is a trait that has previously been described in blunt force trauma [29]. The authors mentioned it to be a great indicator for the impact direction because it was exclusively found at the compression (impact) side. In comparison, we also commonly found it in gunshot trauma, though as an indicator for the exit side. *Stepped breakout* was more frequently seen in femurs than humeri. This might be traced back to the different shapes of the posterior shaft, which is rather edgy in femurs and round in humeri.

General fracture characteristics

This study confirms our previous observation of *plastic deformation* in ballistic long bone trauma [27]. It is often reported that in blunt force trauma, bone acts as viscoelastic material and thus plastic deformation occurs prior to fracture, while in gunshot trauma, bone acts as brittle material and breaks without going through the stage of plastic deformation [36, 42, 60]. Yet, it is also mentioned that limited plastic deformation can occur in gunshot trauma, too [60]. Some authors [11, 25], though, linked this observation to low-velocity ballistic impacts such as the projectiles used in the current study.

With respect to the fracture surface, by using an animal-bovine model, Adharapurapu et al. suggest that it smooths out at increasing impact energies [61]. In our human bone

experimental analysis, however, we noted the fracture surface displayed bone scales, referred to as *fracture surface scaling*. The fracture margin revealed that occasionally superficial bone chips were missing, referred to as *marginal chipping*. In the literature, marginal bone chipping has also been observed in blunt force trauma, named as “knapping” [41]. It was explained that in repeated impacts, the conjoining fractures would rub against each other and cause spalling along the margins. In our study, we saw on the high-speed videos that after the bone fragments are propelled away by the temporary cavity, they are forcefully thrown back again. However, as this trait was observed in the samples without gel too, we assume marginal chipping was rather produced in the course of bullet impact than forceful retraction of the temporary cavity.

Finally, we have observed that the fracture extent was larger in femurs than humeri. This may be related to the bullet’s energy lost upon impact. Our results show that when both bone length and shaft diameter increase, the bone shatters less and the fracture lines propagate longer, which could imply a greater energy loss. In comparison, humeri revealed shorter fractures but a greater fragmentation, as noticed by smaller fragments and greater difficulty in reassembling them. In this context, support is given by the evidence that the grade of fragmentation is linked to the target size [42].

Limitations

The use of human bones for forensic experiments is associated with various limitations due to limited access and difficult tissue handling. Our sample size only allowed us to test one ballistic scenario. It can be assumed that the fracture patterns may differ to varying degrees when the ballistic variables such as bullet calibre, structure, speed and impact angle or the shooting distance are changed. Also, age- and sex-related bone properties may influence the fracture pattern. Furthermore, the results were obtained within an experimental setup using a test barrel and a soft tissue simulant. With respect to the latter, the underlying mechanism of how the gel exactly impacts the fracture pattern has to be further investigated. In concrete, it remains to be revealed whether the varying fracture characteristics are related to a different impact velocity after penetrating a 2-cm-thick gel layer or to another influence that soft tissue has on the bone. Furthermore, previous studies have indicated that Clear Ballistics Gel® cannot be considered equivalent to the standard 10% ballistic gelatine [28]. Authors have reported variations in Clear Ballistics Gel® concerning bullet penetration depth, temporary cavity and peak retarding forces, ultimately failing to meet the FBI calibration criteria [28]. This area warrants further investigation and should be considered in future studies investigating ballistic bone trauma.

Conclusion

With this study, we could define a distinctive ballistic fracture pattern for human long bones. The results have been achieved under the specific circumstance of a perpendicular impact of a 9-mm FMJ bullet shot at a handgun speed from a distance of 2 m. Specifically, a reliable discrimination between bullet entrance and exit was doubtlessly possible allowing to define the bullet's flight direction. The bullet entrance could be identified by a round entry hole with radiating and concentric fractures and several cortical traits such as *v-shape*, *wing piece*, *lateral notch*, *internal beveling*, *ring defect*, *tip fragmentation*, *wing flake defect* and *wing flake*. The exit hole was predominantly square and accompanied by radiating and concentric fractures. It further featured cortical traits such as *external beveling*, *layered breakage* and *stepped breakout*. In addition, general cortical traits such as *plastic deformation*, *fracture surface scaling* and *marginal chipping* were also attributed to ballistic long bone trauma. All evaluated cortical traits were reproduced in both humeri and femurs, leading to the assumption that they may be valid for other long bones, too. However, the trait's occurrence values may considerably differ between the types of bone. In this context, we found that some fracture characteristics correlate with bone properties such as shaft diameter, bone length and cortical thickness. The application of soft tissue simulant in bone trauma experiments was also revealed to influence the fracture pattern, even though the underlying effects require to be further investigated. This study provides new evidences on the ballistic fracture pattern in order to contribute to a clearer guidance on how to identify gunshot trauma when investigating fractured long bones. This is particularly relevant when forensic pathologists and anthropologists deal with skeletal remains that lack correlations with soft tissue findings. Nevertheless, due to the dynamic nature of gunshot incidents, more research is needed to evaluate to which extent the ballistic fracture pattern alters when ballistic variables and bone characteristics change.

Acknowledgements The authors are grateful to the Mossos d'Esquadra for providing the facilities, the material and the personal staff in order to realise the gunshot experiments.

Author contribution Conceptualisation: Nathalie Schwab, Ignasi Galtés; methodology: Nathalie Schwab, Jordi Monreal, Xavier Garrido, Joan Soler, Manel Vega, Pedro Brillas; formal analysis and investigation: Nathalie Schwab, Ignasi Galtés, Xavier Jordana; writing—original draft preparation: Nathalie Schwab; writing—review and editing: Ignasi Galtés, Xavier Jordana, Nathalie Schwab; visualisation: Nathalie Schwab, Ignasi Galtés, Xavier Jordana; supervision: Ignasi Galtés, Xavier Jordana.

Funding Proyectos de Generación de Conocimiento, Agencia Estatal de Investigación (PID2021-124112NB-100). Research Fund for Excellent Junior Researchers of the University of Basel, Switzerland.

Spanish National Plan for Scientific and Technical Research and Innovation, PID2021-124112NB-100, Xavier Jordana, Universität Basel.

Declarations

Ethics approval and consent to participate This study is in accordance with the ethical precepts of the Declaration of Helsinki (Fortaleza, Brazil, October 2013). It was approved by the local ethics committee (Bellvitge University Hospital, L'Hospitalet de Llobregat, Barcelona; Ref. PR416/20). All human bones were handled following the guidance for clinical use (EEC regulations 2004/23/CE and 2006/17/CE) and the legal requirements of Spain (Law 14/2007, RD 1716/2011 and RD 9/2014). The bones were donated anonymously and gathered with informed consent. All used specimens are stored in the private collection at the Catalanian Institute of Legal Medicine and Forensic Science (IMLCFC) in Barcelona, Spain (Registro Nacional de Biobancos. Ref. C.0004241).

Conflict of interest The authors declare no competing interests.

References

- Hart GO (2005) Fracture pattern interpretation in the skull: differentiating blunt force from ballistic trauma using concentric fractures. *J Forensic Sci* 50:JFS2004219
- SA Symes N, Ericka ENC, L'Abbé et al (2012) 17 Interpreting Traumatic A companion to forensic anthropology 39:340
- Schwab CW (1993) Violence: America's uncivil war—presidential address, sixth scientific assembly of the eastern association for the surgery of trauma. *J Trauma* 35:657–665
- Bartlett CS (2003) Clinical update: gunshot wound ballistics. *Clin Orthop Relat Res* 408:28–57
- Saayman G (2006) Gunshot wounds: medico-legal perspectives. *CME: Your SA J CPD* 24:131–136
- Dougherty PJ, Sherman D, Dau N, Bir C (2011) Ballistic fractures: indirect fracture to bone. *J Trauma Acute Care Surg* 71:1381–1384
- Belmont PJ Jr, Goodman GP, Zacchilli M et al (2010) Incidence and epidemiology of combat injuries sustained during “the surge” portion of operation Iraqi Freedom by a US Army brigade combat team. *J Trauma Acute Care Surg* 68:204–210
- Griffiths D, Clasper J (2006) (iii) Military limb injuries/ballistic fractures. *Curr Orthop* 20:346–353
- Dougherty PJ, Vaidya R, Silvertown CD et al (2009) Joint and long-bone gunshot injuries. *JBSJ* 91:980–997
- Najibi S, Dougherty PJ (2006) Management of gunshot wounds to the joints. *Tech Orthop* 21:200–204
- Berryman HE, Symes SA (1998) Recognizing gunshot and blunt cranial trauma through fracture interpretation. *Forensic Osteol* 2:333–352
- O'Be S, Berryman HE, Lahren CH (1987) Cranial fracture patterns and estimate of direction from low velocity gunshot wounds. *J Forensic Sci* 32:1416–1421
- Smith OC, Pope EJ, Symes SA (2015) Look until you see: identification of trauma in skeletal material In: *Hard evidence* Routledge pp 190–204
- Bland-Sutton SJ (1915) Observations on injuries of the bones of the limbs by the S. bullet. *BMJ Mil Health* 24:314–323
- Bir C, Andreacovich C, DeMaio M, Dougherty PJ (2016) Evaluation of bone surrogates for indirect and direct ballistic fractures. *Forensic Sci Int* 261:1–7. <https://doi.org/10.1016/j.forsciint.2016.01.023>
- Huelke DF, Harger JH, Buege LJ et al (1968) An experimental study in bio-ballistics. *J Biomech* 1:97–105. [https://doi.org/10.1016/0021-9290\(68\)90012-2](https://doi.org/10.1016/0021-9290(68)90012-2)
- Huelke DF, Buege LJ, Harger JH (1967) Bone fractures produced by high velocity impacts. *Am J Anat* 120:123–131
- Huelke DF, Harger JH, Buege LJ, Dingman HG (1968) An experimental study in bio-ballistics: femoral fractures produced

- by projectiles—II Shaft impacts. *J Biomech* 1:313–321. [https://doi.org/10.1016/0021-9290\(68\)90025-0](https://doi.org/10.1016/0021-9290(68)90025-0)
19. Ragsdale BD, Josselson A (1988) Experimental gunshot fractures. *J Trauma Acute Care Surg* 28:S109–S115
 20. Robens W, Küsswetter W (1982) Fracture typing to human bone by assault missile trauma. *Acta Chir Scand Suppl* 508:223–227
 21. Coudane H, Grosdidier G, Borrelly J et al (1982) Experimental study of limb lesions due to hunting weapons. *Acta Chir Scand Suppl* 508:229–234
 22. Berryman HE, Gunther WM (2000) Keyhole defect production in tubular bone. *J Forensic Sci* 45:483–487
 23. Long WT, Chang W, Brien EW (2003) Grading system for gunshot injuries to the femoral diaphysis in civilians. *Clin Orthop Relat Res* 408:92–100
 24. Ryan JR, Hensel RT, Saliccioli GG, Pedersen HE (1981) Fractures of the femur secondary to low-velocity gunshot wounds. *J Trauma Acute Care Surg* 21:160–162
 25. Martrille L, Symes SA (2019) Interpretation of long bones ballistic trauma. *Forensic Sci Int* 302:109890. <https://doi.org/10.1016/j.forsciint.2019.109890>
 26. Veenstra A, Kerkhoff W, Oostra R-J, Galtés I (2022) Gunshot trauma in human long bones: towards practical diagnostic guidance for forensic anthropologists. *Forensic Sci Med Pathol* 18:359–367. <https://doi.org/10.1007/s12024-022-00479-0>
 27. Schwab N, Jordana X, Soler J et al (2023) Can Synbone® cylinders and deer femurs reproduce ballistic fracture patterns observed in human long bones? *J Mater Sci* 58:4970–4986. <https://doi.org/10.1007/s10853-023-08333-6>
 28. Courtney E, Courtney A, Andrusiv L, Courtney M (2017) Clear Ballistics Gel®: high speed retarding force analysis of paraffin-based alternative to gelatin-based testing of lead-free pistol bullets. In: 30th International Symposium on Ballistics. DEStech Publications, Inc.
 29. Scheirs S, Malgosa A, Sanchez-Molina D et al (2017) New insights in the analysis of blunt force trauma in human bones Preliminary results. *Int J Legal Med* 131:867–875. <https://doi.org/10.1007/s00414-016-1514-1>
 30. Saukko P, Knight B (2015) Knight's forensic pathology. CRC Press
 31. DiMaio VJM (2015) Gunshot wounds: practical aspects of firearms, ballistics, and forensic techniques, 3rd edn. CRC Press
 32. Kimmerle EH, Baraybar JP (2008) Skeletal trauma: identification of injuries resulting from human rights abuse and armed conflict. CRC Press
 33. Andrews P, Fernández-Jalvo Y (2012) How to approach perimortem injury and other modifications. In: Bell LS (ed) *Forensic Microscopy for Skeletal Tissues*. Humana Press, Totowa, NJ, pp 191–225
 34. Kieser DC, Riddell R, Kieser JA, et al (2014) Bone micro-fracture observations from direct impact of slow velocity projectiles. *J Arch Mil Med* 2. <https://doi.org/10.5812/jamm.15614>
 35. Leffers D, Chandler RW (1985) Tibial fractures associated with civilian gunshot injuries. *J Trauma* 25:1059–1064
 36. Dirkmaat D (2012) A companion to forensic anthropology. John Wiley & Sons
 37. Cohen H, Kugel C, May H et al (2016) The impact velocity and bone fracture pattern: forensic perspective. *Forensic Sci Int* 266:54–62. <https://doi.org/10.1016/j.forsciint.2016.04.035>
 38. Messerer O (1880) Über Elasticität und Festigkeit der menschlichen Knochen. Cotta
 39. Symes SA, L'Abbé EN, Chapman EN, et al (2012) Interpreting traumatic injury to bone in medicolegal investigations. In: A companion to forensic anthropology John Wiley & Sons Ltd pp 340–389
 40. Christensen AM, Passalacqua NV, Bartelink EJ (2019) Forensic anthropology: current methods and practice. Academic Press
 41. Klepinger LL (2006) Fundamentals of forensic anthropology. John Wiley & Sons
 42. Kieser J, Taylor M, Carr D (2012) Forensic Biomechanics. John Wiley & Sons
 43. Baraybar JP, Gasior M (2006) Forensic anthropology and the most probable cause of death in cases of violations against international humanitarian law: an example from Bosnia and Herzegovina. *J Forensic Sci* 51:103–108
 44. Besant-Matthews PE (2000) Examination and interpretation of rifled firearm injuries The pathology of trauma, 3rd edn Arnold, London 47–60
 45. Sauer NJ (1998) The timing of injuries and manner of death: distinguishing among antemortem, perimortem and postmortem trauma. *Forensic Osteol* 2:321–331
 46. Steadman DW, Basler W, Hochrein MJ, et al (2016) Domestic homicide investigations: an example from the United States. In: *Handbook of Forensic Anthropology and Archaeology*. Routledge, pp 351–362
 47. Quatrehomme G, Işcan MY (1998) Analysis of beveling in gunshot entrance wounds. *Forensic Sci Int* 93:45–60. [https://doi.org/10.1016/S0379-0738\(98\)00030-9](https://doi.org/10.1016/S0379-0738(98)00030-9)
 48. Berryman HE, Smith OC, Symes SA (1995) Diameter of cranial gunshot wounds as a function of bullet caliber. *J Forensic Sci* 40:751–754
 49. Paschall A, Ross AH (2017) Bone mineral density and wounding capacity of handguns: implications for estimation of caliber. *Int J Legal Med* 131:161–166. <https://doi.org/10.1007/s00414-016-1420-6>
 50. Ross AH (1996) Caliber estimation from cranial entrance defect measurements. *J Forensic Sci* 41(4):629–633
 51. Tamáska L (1964) Kritische Bemerkungen zur Frage der Geschosskaliberbestimmung aus dem Durchmesser der Einschussöffnungen der Knochen. *Zacchia* 39:158–170
 52. Pollak S, Ritt F (1992) Vergleichende Untersuchungen an Einschusslücken in Rumpf- und Extremitätenknochen mit vorwiegend spongioser Struktur. *Beitr Gerichtl Med* 50:363–363
 53. Spitz WU, Fisher RS (1980) *Medicolegal Investigation of Death*, Charles C. Thomas, Springfield, IL
 54. Coe JI (1982) External beveling of entrance wounds by handguns. *Am J Forensic Med Pathol* 3:215
 55. Baik S-O, Uku JM, Sikirica M (1991) A case of external beveling with an entrance gunshot wound to the skull made by a small caliber rifle bullet. *Am J Forensic Med Pathol* 12:334–336
 56. Peterson BL (1991) External beveling of cranial gunshot entrance wounds. *J Forensic Sci* 36:1592–1595
 57. Madea B, Staak M (1988) Determination of the sequence of gunshot wounds of the skull. *J Forensic Sci Soc* 28:321–328
 58. Huelke DF, Darling JH (1964) Bone fractures produced by bullets. *J Forensic Sci* 9:461–469
 59. Quatrehomme G, Yaşar Işcan M (1997) Beveling in exit gunshot wounds in bones. *Forensic Sci Int* 89:93–101. [https://doi.org/10.1016/S0379-0738\(97\)00121-7](https://doi.org/10.1016/S0379-0738(97)00121-7)
 60. Wedel VL, Galloway A (2013) Broken bones: anthropological analysis of blunt force trauma (2nd Ed.). Charles C Thomas Publisher
 61. Adharapurapu RR, Jiang F, Vecchio KS (2006) Dynamic fracture of bovine bone. *Mater Sci Eng, C* 26:1325–1332

Publisher's Note Springer Nature remains neutral with regard to jurisdictional claims in published maps and institutional affiliations.

Springer Nature or its licensor (e.g. a society or other partner) holds exclusive rights to this article under a publishing agreement with the author(s) or other rightsholder(s); author self-archiving of the accepted manuscript version of this article is solely governed by the terms of such publishing agreement and applicable law.